New Type of Charged Defect in Amorphous Chalcogenides

S. I. Simdyankin,[1,*] T. A. Niehaus,[2] G. Natarajan,[1] Th. Frauenheim,[2] and S. R. Elliott[1]
[1]*Department of Chemistry, University of Cambridge, Lensfield Road, Cambridge CB2 1EW, United Kingdom*
[2]*Fachbereich 6 - Theoretische Physik, Universität Paderborn, Warburger Straße 100, D-33098, Paderborn, Germany*

(Received 17 September 2004; published 2 March 2005)

We report on density-functional-based tight-binding simulations of a series of amorphous arsenic sulfide models. In addition to the charged coordination defects previously proposed to exist in chalcogenide glasses, a novel defect pair, $[As_4]^-$-$[S_3]^+$, consisting of a fourfold coordinated arsenic site in a seesaw configuration and a threefold coordinated sulfur site in a near-planar trigonal configuration, was found in several models. The valence-alternation pairs $[S_3]^+$-$S_1{}^-$ are converted into $[As_4]^-$-$[S_3]^+$ pairs under HOMO-to-LUMO electronic excitation. This structural transformation is accompanied by a decrease in the size of the HOMO-LUMO band gap, which suggests that such transformations could contribute to photodarkening in these materials.

DOI: 10.1103/PhysRevLett.94.086401 PACS numbers: 71.23.Cq, 61.43.Dq

Amorphous chalcogenides, i.e., sulfides, selenides, and tellurides, are distinguished from other materials by their photosensitivity. These materials exhibit intriguing photoinduced phenomena that are not observed in their crystalline counterparts. Some of these unusual phenomena have many potential applications [1]. A detailed microscopic understanding of the origin of these phenomena [2], however, is still lacking.

In the context of photoinduced structural changes, special significance is attributed to the presence of oppositely charged coordination-defect (valence-alternation) pairs [3]. Normally, such defect pairs contain singly coordinated chalcogen atoms having distinct spectroscopic signatures [3]. Experimentally, the concentration of these defects is estimated to be rather small [4], i.e., 10^{17} cm^{-3}, compared with the atomic density of about 2×10^{25} cm^{-3}, in order quantitatively to account for the observed magnitude of the photoinduced effects.

We have investigated the structure of, and simulate photostructural changes in, a series of computer-generated models of the archetypal amorphous chalcogenide, diarsenic trisulfide (a-As_2S_3). In addition to the well-known [3] valence-alternation pairs (VAPs) $[C_3]^+$-$C_1{}^-$ and $P_4{}^+$-$C_1{}^-$, where C_n/P_n stands for an n-fold coordinated chalcogen/pnictogen (e.g., sulfur/arsenic) atom, some of the models were found to contain the previously unreported $[P_4]^-$-$[C_3]^+$ defect pairs. These are unusual in two ways. First, there is an excess of *negative* charge in the vicinity of the normally electropositive pnictogen atoms and, second, there are no undercoordinated atoms with dangling bonds in these local configurations. The latter peculiarity may be the reason why such defect pairs have not yet been identified experimentally.

All our simulations have been done using a density-functional-based tight-binding (DFTB) method [5], unless specified otherwise. We found that a basis set of s, p, and d Slater-type orbitals for all atoms is an essential prerequisite for the observation of the defect-related effects reported here [6]. Each of the models contained 60 (24 As and 36 S) atoms. This size of model was chosen so as to be big enough that the defect pairs could be accommodated within the volume of the periodic simulation box, and yet small enough to allow for the creation and analysis of several statistically independent models in a reasonable time. The quality of the models, in terms of comparison with experimental neutron-diffraction data, is similar to that of the larger models reported in Ref. [7].

By using *NVT* (constant number of particles, volume, and temperature) molecular-dynamics simulations, we created a supercell 24-atom model of amorphous arsenic by quenching from the melt. Threefold coordination was imposed by iteratively modifying the nearest-neighbor shell of each atom and bringing the system to thermal equilibrium at room temperature. A stoichiometric model (model 0, in the following) of a-As_2S_3 was then created by decorating each of the As-As bonds with S atoms, followed by rescaling the model to the experimental density [8] $\rho = 3.186$ g/cm^3 and relaxing at room temperature ($T = 300$ K). This model was then melted at $T = 3000$ K and ten more models were created by taking snapshots of the 3000 K molecular-dynamics trajectory at irregular time intervals as starting configurations, and following the cooling schedule described in Ref. [7].

The defect statistics for the models containing coordination defects are shown in Table I. The coordination numbers were calculated as the number of nearest neighbors within a spherical shell of a radius corresponding to the position of the first minimum in the corresponding partial radial distribution function. The numbers in each triplet in Table I show the number of corresponding defects in (I) the as-prepared ground-state optimized geometry, (II) the excited-state geometry optimized under the constraint of having one electron in the highest occupied molecular orbital (HOMO) and one electron in the lowest unoccupied molecular orbital (LUMO), and (III) the ground-state optimized geometry obtained from the

TABLE I. Defect statistics for the models containing coordination defects. Each triplet of numbers denotes (I) the number of defects in the as-prepared ground state, (II) the HOMO-LUMO-promoted excited state, and (III) the ground state resulting from the excited state.

Model	Number of coordination defects				homopolar bonds	
	As_2	As_4	S_1	S_3	As-As	S-S
0	0,1,0	0,0,0	0,1,0	0,0,0	0,0,0	0,0,0
1	0,1,0	1,1,1	0,0,0	1,0,1	1,1,1	1,1,1
2	0,2,0	0,0,1	1,0,0	1,0,1	2,1,2	2,2,2
3	0,0,0	1,1,1	1,1,1	0,0,0	1,1,1	0,0,0
5	0,0,0	0,0,0	0,1,0	0,0,0	1,1,1	1,0,1
6	0,0,0	1,0,1	0,1,0	1,1,1	2,2,2	2,2,2
10	0,1,0	0,0,1	1,0,0	1,1,1	1,0,1	1,1,1

excited-state configuration. Although electronic excitations where one electron is promoted from HOMO-to-LUMO Kohn-Sham states [9] are not especially realistic, we simulate such excitations in order qualitatively to assess defect stability with respect to (optically induced) electronic excitations. Note that in models two and 10, S_3-S_1 defect pairs converted into As_4-S_3 pairs as a result of the electronic excitation.

The statistics of Mulliken charges (in atomic units) were calculated for all 11 models in the ground state before and after electronic excitation. Since all extremal charge values, which significantly deviate from the average values (0.32 for As, -0.21 for S), correspond to coordination defects, these data confirm that the coordination defects form charged defect pairs. The maximum positive charge (0.46) is on a fourfold coordinated As atom that is part of an intimate valence-alternation pair (IVAP) where a singly coordinated S atom is covalently bonded to it. The minimum positive charge (0.07) is on an As atom that forms a homopolar bond with an As_4 center (see Table II). The minimum negative charge (-0.36) is on a singly coordinated S atom, and the maximum negative charge (-0.03) is on a S atom that forms a homopolar bond with another S atom with a similar charge value.

It is common [3] to use the following notation for VAPs: ${As_4}^+$-${S_1}^-$ and ${S_3}^+$-${S_1}^-$, where the superscripts show the polarity of the nominal excess charge on corresponding defect centers. Although the charges on As_4 and S_1 atoms are of correct polarity in an alloy of normally electropositive As and electronegative S, those on S_3 are not. Therefore, it is more appropriate to use the notation $[S_3]^+$ for threefold coordinated S atoms, where the square brackets imply that the excess charge is distributed between the center and its nearest neighbors. Table II shows that there is also an excess negative charge in the vicinity of As_4 centers when $[S_3]^+$ centers are also present, and these newly identified defects will be denoted as $[As_4]^-$ here.

It is of interest to verify whether the excess charge has a similar effect on the local structure in both supercell amorphous and isolated cluster models. Figure 1(a) shows a fragment of model 2(III) containing both $[As_4]^-$ and $[S_3]^+$ defects. Figure 1 also shows the optimized geometry in (b) $[SAs_3H_6]^+[$ and (c) $[AsS_4H_4]^-$ clusters, where one electron was removed from and added to the neutral system, respectively. The seesaw $[As_4]^-$ and planar $[S_3]^+$ local configurations observed in models 1(I), 2(III) [see Fig. 1(a)], 6(I) and 10(III) are indeed very similar to those in the isolated clusters shown in Figs. 1(b) and 1(c), respectively. We note that similar seesawlike structures are also observed in local configurations around hypervalent chalcogens, e.g., in sulfur(IV) fluoride and in certain tellurites [10], and are expected from stereochemical considerations [11]. Also, the fivefold coordinated As defect reported in [12] can be viewed as an $[As_4]^-$ center bonded to an additional As atom [placed on top of the structure

TABLE II. Mulliken charges, in atomic units, on atoms within the $[As_4]^-$-$[S_3]^+$ defect pairs. The index (I) next to the model number signifies the as-prepared ground-state geometry, and (III) indicates the ground-state structure obtained by geometry optimization of the excited-state configuration (II). The relevant fragment of model 2(III) and the clusters $[SAs_3H_6]^+$ and $[AsS_4H_4]^-$ are depicted in Figs. 1(a)–1(c), respectively.

Model	Center	Neighbors				Total
		1	2	3	4	
1(I)	(As) 0.313	(S) -0.194	(S) -0.281	(S) -0.223	(S) -0.313	-0.698
	(S) -0.110	(As) 0.363	(As) 0.379	(As) 0.362		0.994
2(III)	(As) 0.329	(As) 0.071	(S) -0.221	(S) -0.203	(S) -0.329	-0.353
	(S) -0.153	(As) 0.355	(As) 0.347	(As) 0.351		0.900
6(I)	(As) 0.345	(S) -0.149	(S) -0.255	(S) -0.295	(S) -0.225	-0.579
	(S) -0.146	(As) 0.375	(As) 0.376	(As) 0.384		0.989
10(III)	(As) 0.326	(As) 0.101	(S) -0.242	(S) -0.308	(S) -0.231	-0.354
	(S) -0.158	(As) 0.363	(As) 0.295	(As) 0.101		0.601
$[AsS_4H_4]^-$	(As) 0.280	(S) -0.359	(S) -0.320	(S) -0.498	(S) -0.600	-1.497
$[SAs_3H_6]^+$	(S) -0.149	(As) 0.365	(As) 0.362	(As) 0.374		0.952

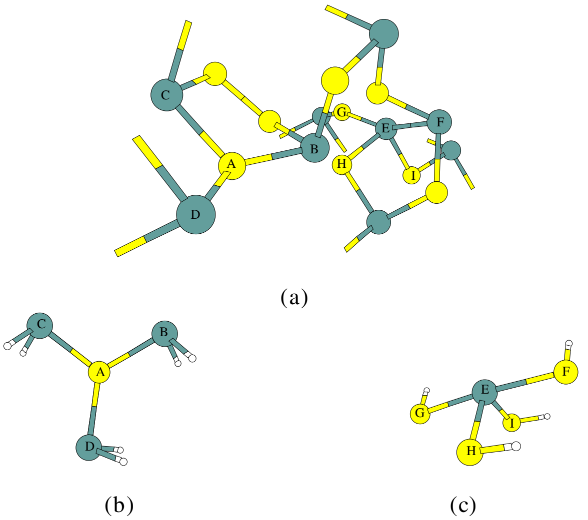

FIG. 1 (color online). Planar trigonal, $[S_3]^+$ (marked by letter A), and seesaw, $[As_4]^-$ (marked by letter E), configurations in (a) a fragment of model 2(III) [the dangling bonds show where the displayed configuration connects to the rest (not shown) of the network], and (b), (c) charged isolated clusters (the dangling bonds are terminated with hydrogen atoms). The shading of the As atoms is darker than that of the S atoms. Bond lengths are (Å) as follows: (a) $AB = AD = 2.42$, $AC = 2.39$, $EF = 2.83$, $EG = 2.54$, $EH = 2.35$, $EI = 2.33$; (b) $AB = 2.34$, $AC = AD = 2.33$; (c) $EF = 2.55$, $EG = 2.46$, $EH = 2.30$, $EI = 2.32$.

depicted in Fig. 1(c)]. It is also worth mentioning that there is a distinct pattern in the distribution of charges in the seesaw configuration, which is most clearly seen in the isolated $[AsS_4H_4]^-$ cluster: the more distant sulfur atoms F and G [see Fig. 1(c)] have the largest magnitude negative charges (see Table II). While the $[As_4]^-$ centers in models 1(I) and 6(I) are both chemically and topologically identical to the corresponding center in the $[AsS_4H_4]^-$ cluster, the respective centers in models 2(III) and 10(III) are different in that they both contain As-As homopolar bonds, which makes them less negative. Interestingly, five-membered rings fit conveniently to parts of the overcoordinated defect centers in models 2(III) (both $[As_4]^-$ and $[S_3]^+$) and 10(III) (only $[As_4]^-$), which might contribute to the stability of this type of defect pair. These rings containing $[As_4]^-$ centers may have distinct vibrational frequencies, which can be exploited in an attempt to detect these centers experimentally.

Although the DFTB method involves a number of approximations, it has been shown [5] that its accuracy is comparable with that of full DFT methods. We verified that the $[As_4]^-$-$[S_3]^+$ defect pair is reproducible with more accurate methods.

We have found that the hitherto unreported $[As_4]^-$-$[S_3]^+$ defect pairs in our models are stable with respect to HOMO-to-LUMO electron excitations. We also performed a geometry optimization of an $As_4S_{10}H_8$ cluster, containing an $[As_4]^-$-$[S_3]^+$ pair by construction, both in the ground state and in the first singlet excited state within the linear-response approximation to time-dependent density-functional theory, which gives a much better description of excited states compared with HOMO-to-LUMO electron excitations [13] (see Fig. 2). Although the bond AC in the ground-state structure depicted in Fig. 2(a) is significantly elongated, analysis of the electron density in the HOMO and LUMO electronic states [see Fig. 2(b)] shows that it has a significant bonding character, implying that this cluster contains a distorted $[As_4]^-$-$[S_3]^+$ pair. As seen in Fig. 2(c), redistribution of the electron density in the excited state leads to a symmetrization of the As_4 center and to an elongation of the bond BE in the region of the S_3 center, where the LUMO electronic state is predominantly localized. Subsequent geometry optimization of the excited-state configuration results in the same ground-state geometry as in Fig. 2(a). We observed that bond breaking/elongation in all our models generally occurs at the groups of atoms where the LUMO is localized, indicating the expected antibonding character of LUMO states.

The HOMO-LUMO band-gap energies for models 0–10 are listed in Table III. The three values correspond to the same ground-state, excited-state, ground-state geometries as in Table I. Note that in models 2 and 10, the magnitude of the band-gap decreases as $[S_3]^+$-$S_1{}^-$ pairs are converted

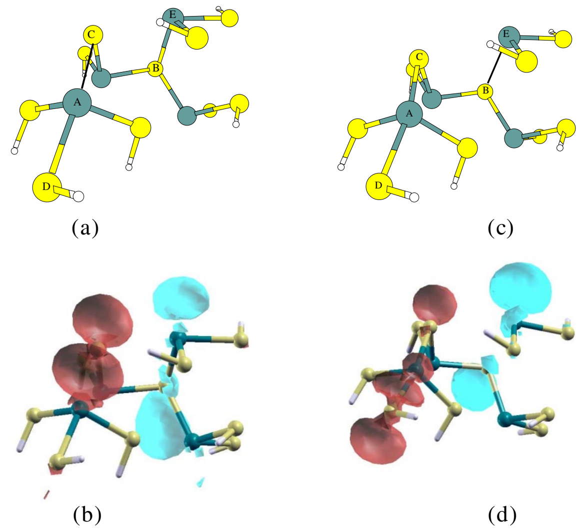

FIG. 2 (color online). An $As_4S_{10}H_8$ cluster containing both defect centers $[As_4]^-$ (marked by letter A) and $[S_3]^+$ (marked by letter B). The shading of the atoms is the same as in Fig. 1. The black solid lines signify elongated bonds. (a) Optimized ground-state geometry. Bond lengths are (Å) as follows: $AC = 3.00$, $AD = 2.32$, and $BE = 2.4$. (b) Isosurfaces corresponding to the value of 0.025 of electron density in the HOMO [darker surface, left side, (red online)] and LUMO [lighter surface, right side (cyan online)] states for the structure shown in (a). (c) Optimized geometry in the first singlet excited state. Bond lengths are (Å) as follows: $AC = 2.43$, $AD = 2.44$, and $BE = 2.82$. (d) Same as (b), but for the structure shown in (c).

TABLE III. HOMO-LUMO band-gap energies for the all-heteropolar model 0 and the models containing coordination defects. The indices (I), (II), and (III) correspond to the triplets in Table I.

Model	Band-gap (eV)		
	(I)	(II)	(III)
0	1.46	0.68	1.46
1	1.13	0.94	1.13
2	1.41	0.62	1.06
3	1.23	0.21	1.24
4	1.47	1.50	1.47
5	1.68	0.40	1.67
6	1.47	1.37	1.47
7	1.47	1.50	1.47
8	1.38	1.20	1.38
9	1.65	1.31	1.65
10	1.20	0.85	1.02

into $[\mathrm{As}_4]^-$-$[\mathrm{S}_3]^+$ pairs. It should be noted that $[\mathrm{S}_3]^+$ centers are not necessarily conserved under such conversions—while in model 10 the S_3 atom is the same in both ground states (I) and (III), in model 2 it is not.

The fact that $[\mathrm{As}_4]^-$-$[\mathrm{S}_3]^+$ pairs are stable, both in periodic supercell (with respect to thermal fluctuations for about 100 ps at $T = 300$ K) and isolated cluster (with respect to excited-state optimization) models, suggests that this model of new charged defect pairs should apply equally to photoinduced phenomena in both bulk and thin films of this material. The possible presence of these defect centers is consistent with experimental observation of low-energy vibrational excitations in a-$\mathrm{As}_2\mathrm{S}_3$ films [14]. Excess low-energy excitations can be attributed to tunneling between "umbrellalike" vibrations of the nearly planar $[\mathrm{S}_3]^+$ centers (as in the corresponding motion in NH_3, responsible for its maser action).

In summary, we have demonstrated the existence of a new type of charged defect pair in amorphous arsenic sulfide, namely $[\mathrm{As}_4]^-$-$[\mathrm{S}_3]^+$, where the As center has a "seesaw" configuration, and the S center is trigonal planar. A plausible scenario for photodarkening in this material is the conversion of other types of defects containing under-coordinated atoms into such defect pairs due to electronic excitation under illumination. Interestingly, in the two models where such conversion has been observed, As-As homopolar bonds were formed as part of the $[\mathrm{As}_4]^-$ centers. Given that such bond lengths are greater than the average bond length in the material, such bond formation could also contribute to photoexpansion of the material.

S. I. S. and G. N. are grateful to the EPSRC for financial support. We thank the British Council and DAAD for provision of financial support. We used the XMAKEMOL [15] and XCRYSDEN [16] software for visualization.

---

*Electronic address: sis24@cam.ac.uk

[1] *Chalcogenide Glasses and Sol-Gel Materials*, Handbook of Advanced Electronic and Photonic Materials and Devices Vol. 5, edited by H. S. Nalwa (Academic Press, San Diego, 2001).

[2] *Photo-Induced Metastability in Amorphous Semiconductors*, edited by A. V. Kolobov (Wiley-VCH, Weinheim, 2003).

[3] M. Kastner, D. Adler, and H. Fritzsche, Phys. Rev. Lett. **37**, 1504 (1976).

[4] A. Feltz, *Amorphous Inorganic Materials and Glasses* (VCH, Weinheim, 1993), p. 203.

[5] T. Frauenheim, G. Seifert, M. Elstner, T. Niehaus, C. Köhler, M. Amkreutz, M. Sternberg, Z. Hajnal, A. D. Carlo, and S. Suhai, J. Phys. Condens. Matter **14**, 3015 (2002).

[6] S. I. Simdyankin, S. R. Elliott, T. A. Niehaus, and T. Frauenheim, in *Computational Modeling and Simulation of Materials III*, edited by P. Vincenzini, A. Lami, and F. Zerbetto (Techna Group s.r.l., Faenza, Italy, 2004), vol. A, p. 149.

[7] S. I. Simdyankin, S. R. Elliott, Z. Hajnal, T. A. Niehaus, and T. Frauenheim, Phys. Rev. B **69**, 144202 (2004).

[8] J. H. Lee, A. C. Hannon, and S. R. Elliott, cond-mat/0402587.

[9] X. Zhang and D. A. Drabold, Phys. Rev. Lett. **83**, 5042 (1999).

[10] J. C. McLaughlin, S. L. Tagg, J. W. Zwanziger, D. R. Haeffner, and S. D. Shastri, J. Non-Cryst. Solids **274**, 1 (2000).

[11] M. North, *Principles and Applications of Stereochemistry* (Stanley Thornes, Cheltenham, 1998).

[12] T. Uchino, D. C. Clary, and S. R. Elliott, Phys. Rev. Lett. **85**, 3305 (2000).

[13] T. A. Niehaus, S. Suhai, F. D. Sala, P. Lugli, M. Elstner, G. Seifert, and T. Frauenheim, Phys. Rev. B **63**, 085108 (2001).

[14] J. Honolka, G. Kasper, and S. Hunklinger, Europhys. Lett. **57**, 382 (2002).

[15] M. P. Hodges, Xmakemol homepage, http://www.nongnu.org/xmakemol/.

[16] A. Kokalj, J. Mol. Graphics Mod. **17**, 176 (1999); code available from http://www.xcrysden.org/.